First-principles study of the adsorption of NH_3 on Ag surfaces

M. G. Stachiotti
Instituto de Física Rosario, Universidad Nacional de Rosario, 27 de Febrero 210 Bis, (2000) Rosario, Argentina
(Received 19 August 2008; revised manuscript received 15 December 2008; published 5 March 2009)

Ab initio density-functional theory has been used to investigate the adsorption of NH_3 molecules on Ag(111), (001), and (110) surfaces. Preferred adsorption sites, adsorption energies, and the relaxation of the surface structure were calculated using the all-electron full-potential linearized augmented plane wave method. We find that NH_3 binds preferentially at a top site with the C_3 axis normal to the surface. At this site, the N-Ag distance is practically the same for every surface, while the adsorption energy depends on the surface structure: 0.32, 0.40, and 0.49 eV per molecule for (111), (001), and (110), respectively. Additionally, the electronic structure and binding energies of NH_3Ag_n $(n=1,2)$ complexes have been calculated to investigate to what extent the formation of the weak N-Ag chemical bond might be determined mainly by local interactions. The bonding mechanism is explained as resulting from the combined effects of covalent and polarization contributions.

DOI: 10.1103/PhysRevB.79.115405 PACS number(s): 68.43.Fg

I. INTRODUCTION

The study of adsorbates on metal surfaces has become of central interest in surface science because of the enormous importance of catalysis for industrial applications. These experimental studies can be complemented with simulations which are nowadays a powerful tool for the theoretical description of surface structures and chemical reactions at surfaces because of the growth in computational power and the success of density-functional calculations.[1] In order to understand many of these reactions, it is essential to establish a fundamental knowledge of how atoms and molecules interact with surfaces. The nature of the surface chemical bond will determine the properties and reactivity of the adsorbed molecule.

In nanotechnology, the chemistry at a nanoparticle surface is a key for introducing metal nanoparticles in a variety of matrices. Surface modification by adsorbed molecules makes nanoparticles compatible with a host matrix. For example, colleagues of our laboratory have developed a route for the synthesis of Ag nanoparticles where aminosilane molecules act as surface modifiers, inhibiting particle growth and avoiding aggregation.[2,3] However, the binding mechanism and the effects of these adsorbed molecules on the Ag nanoparticles properties are unknown. In order to understand many of these effects, it is essential to establish a fundamental knowledge of how these molecules interact with Ag surfaces. When a molecule is adsorbed, new electronic states are formed due to the bonding to the surface. Aminosilanes are large and complex molecules;[2] therefore, large molecules can often be viewed as built from different functional groups even if they are joined together by molecular bonds of strength comparable to the intramolecular bonds within the respective building units. By using the bond-prepared functional groups as a starting point, new electronic states appearing in the more complex molecules can be accounted for. Thus, in order to be able to address questions regarding reactivities of complex molecules on metal surfaces, a detailed knowledge about the chemically important functional groups of the system can be very helpful. For example, the adsorption of a single ammonia (NH_3) molecule on Ag surfaces is of particular interest since it provides an adsorbate-substrate interaction via an amino group. The NH_3/Ag system is also interesting for low-temperature selective catalytic oxidation of ammonia. It was reported that silver is a very active ammonia oxidation catalyst, and at low temperatures the performance of supported silver catalysts is even superior to noble-metal catalysts in both selectivity and activity.[4]

The interaction between ammonia and transition and noble metals has been studied extensively over the years and has given rise to a number of interpretations. Based on both theoretical and experimental data, it is generally accepted that chemical bonding in the NH_3-metal system can be related to the occupied $3a1$ (lone-pair) orbital in NH_3 interacting with the metal valence bands. However, while this simple line of reasoning regarding the covalent bond might hold for some metals it is certainly not true for all. For instance, both the position and population of the metal valence bands are crucial in the bond formation. In noble metals, the *d*-band position implies that both the bonding and antibonding $3a1$ hybrids will be occupied.

The question of what governs the bonding between molecular amino groups and noble-metal surfaces is still under debate. In the case of NH_3 adsorbed on copper surfaces there exist a large number of both experimental and theoretical studies.[5–14] Most of the theoretical works have been devoted to the interaction in terms of the electronic structure and the electrostatic and covalent contributions to the adsorption energy. The main findings of some studies are that the predominant contribution to the adsorption energy is due to the electrostatic interaction between the large dipole moment of free NH_3 and the copper surface with smaller covalent contributions involving mainly the ammonia $3a1$ lone-pair orbital.[8,12] Other studies indicated a significant covalent contribution to the bonding,[13,14] showing that the adsorption energy cannot be simulated by a simple electrostatic model. In a recent paper, the bond formed between the amino group of adenine and the Cu(110) surface has been investigated and explained as resulting from the combined effects of electrostatic and strain contributions.[15]

Regarding the adsorption of NH_3 on Ag surfaces, accurate total-energy and electronic-structure calculations are missing. Prior works provided some trends for the binding

mechanism by investigating the NH_3 molecule chemisorbed to a single atom,[16,17] to Ag_2,[18] or to small Ag_{10} and Ag_{16} clusters,[19] arguing that metal cluster-ligand complexes share common features with the adsorbed state at metal surfaces. In this paper we provide quantitative information for the preferred adsorption sites, relaxation of the surface structure, and adsorption energies of a single NH_3 molecule adsorbed on Ag(111), (001), and (110) surfaces. We also investigate to what extent the formation of a N-Ag chemical bond might be determined only by local covalent contributions.

II. COMPUTATIONAL METHOD

The calculations have been performed using density-functional theory (DFT) within the generalized gradient approximation (GGA). We used GGA because gradient corrections become important for the calculation of the properties of adsorbates due to large charge-density inhomogeneities.

For comparison, the properties of the clean surfaces were also evaluated within the local-density approximation (LDA). For the GGA functional, we use the formulation proposed by Perdew *et al.*,[20] which is commonly called Perdew-Burke-Ernzerhof (PBE). The Kohn-Sham equations are solved using the all-electron full-potential linearized augmented plane-wave (FP-LAPW) method,[21] as implemented in the WIEN2K code.[22] This implementation includes total-energy and atomic force calculations, which allows a structural optimization with reverse-communication trust-region quasi-Newton routine from the port library. The core states are treated fully relativistically, while the semicore and valence states are treated by the scalar relativistic approximation. The FP-LAPW wave functions in the interstitial region are represented using a plane-wave expansion truncated to include only plane waves that have kinetic energies less than some particular cutoff energy E^{wf} and for the potential representation in the interstitial region, plane waves with kinetic energies up to E^{pot} are considered. Inside the muffin-tin spheres with radius R_{mt}, the wave functions are expanded in radial functions (solution of the radial Schrödinger equation) times spherical harmonics up to $l_{\mathrm{max}}^{\mathrm{wf}}$, and for the representation of the potential inside the muffin-tin spheres, a maximum of $l_{\mathrm{max}}^{\mathrm{pot}}$ is used. In the present work $E^{\mathrm{wf}}=17.3$ Ry; $R_{\mathrm{mt}}=2.2$ a.u. (Ag), 1.1 a.u. (N), and 0.6 a.u. (H); $l_{\mathrm{max}}^{\mathrm{wf}}=10$; $E^{\mathrm{pot}}=144$ Ry (LDA) and 400 Ry (GGA); and $l_{\mathrm{max}}^{\mathrm{pot}}=6$.

In the calculations we used a supercell geometry. The metal substrate is modeled by a slab of five atomic layers which are separated by a 12-Å-thick vacuum region. The adsorbed NH_3 molecules are placed on only one side of the slab. A $p2\times2$ periodicity is employed in the lateral directions, which shows under tests that artificial molecule-molecule interaction is sufficiently weak and in fact negligible for the questions of concern. The equilibrium NH_3/Ag slab configuration is determined by relaxing the adsorbed molecule and the two top surface layers. The optimized geometries are identified by the requirement that the remaining forces acting on the atoms are smaller than 0.05 eV/Å. The convergence of surface properties with respect to the number of k points and cutoff energy has been carefully tested. For the **k** integration we used 36 uniformly spaced points in the two-dimensional Brillouin zone corresponding to the $p2\times2$ surface unit cell.

In addition to the calculations for the extended model, the local interaction of a NH_3 molecule bonded to one and two Ag atoms ($AgNH_3$ and Ag_2NH_3 complexes) was studied within the DFT formalism by using the LAPW method. These calculations are useful for the physical interpretation of the adsorption mechanism. The equilibrium configuration and total energies of isolated Ag atom, NH_3 molecule, and Ag_nNH_3 complexes are calculated in a cubic cell of side length 16 Å with the **k** point (0,0,0) for the Brillouin-zone sampling. The spin-polarization corrections have been included.

III. RESULTS AND DISCUSSION

A. Clean silver surfaces and isolated NH_3 molecule

The Ag surfaces are the reference systems for this study. The in-plane lattice parameter of the supercells has been set equal to the bulk value. In particular, GGA gives an equilibrium bulk lattice parameter $a_o=4.13$ Å, a bulk modulus $B=93$ GPa, and a cohesive energy $E_c=2.52$ eV per atom. LDA predicts $a_o=4.00$ Å, $B=145$ GPa, and $E_c=3.63$ eV per atom. The experimental values for these quantities are $a_o=4.07$ Å, $B=102$ GPa, and $E_c=2.95$ eV per atom. These results are compatible with previous DFT calculations.[23–26] The tendency of the LDA is to overbind, resulting in a short lattice constant, too high bulk modulus, and too high binding energy. The GGA improves the binding energy and bulk modulus, while the deviation of the lattice constant is similar to that in the LDA (with opposite sign however).

To test the accuracy of the setup proposed for the NH_3/Ag system, we first compute some properties of the separate components. Although the properties of clean Ag surfaces have been reported using different *ab initio* approaches (mainly pseudopotentials), it is useful to compare those results and experimental data with the all-electron calculations. Table I summarizes the GGA results for the (111), (110), and (001) clean surfaces. LDA values are presented also for comparison. As test calculations, surface relaxations and work functions of clean surfaces were computed. The calculated GGA work functions for the (111), (001), and (110) surfaces were 4.43, 4.23, and 4.15 eV, respectively. These values are in accord with the experimental trend: the close-packed (111) surface has the highest work function of 4.48 eV while the open (110) has the lowest work function of 4.14 eV among the low-index silver surfaces. The quantitative agreement between the calculated and experimental values is very good.

Table I also shows the results of the surface relaxation. The change in the interlayer distance is defined as $\Delta d_{ij}=(d_{ij}-d_0)/d_0$, where d_{ij} is the spacing between layers i and j and d_0 is the interlayer spacing in the bulk. The three surfaces show an inward relaxation of the top layer. While no significant structural relaxation is found for the (111) surface ($\Delta d_{12}=-0.2\%$), the (001) surface shows a slightly more relaxed geometry ($\Delta d_{12}=-1.6\%$). The (110) surface presents a stronger reduction in the interlayer distance $\Delta d_{12}=-7.7\%$. In summary, the calculated clean surface properties are in very

TABLE I. LAPW results for the surface interlayer relaxation ($\Delta d_{12}, \Delta d_{23}$) and work function ($\Phi$) for clean Ag surfaces. Experimental data and other *ab initio* results are given for comparison.

		Δd_{12} (%)	Δd_{23} (%)	Φ (eV)
Ag(111)	GGA	−0.2	−0.6	4.43
	LDA	−1.0	−0.7	4.84
	Expt.	$<\|2\|$[a]	0.6[b]	4.48[c]
		No relaxation[d]		
		−0.5[e]		
	LDA[f]	−1.4		4.67
	GGA[g]	−0.5	−0.5	4.55
Ag(110)	GGA	−7.7	2.8	4.15
	LDA	−8.5	2.2	4.58
	Expt.	-7.8 ± 2.5[h]	4.3 ± 2.5[h]	4.14 ± 0.04[c]
		−5.7[i]	2.2[i]	
	LDA[f]	−3.6		4.23
	GGA[g]	−10.2	4.8	4.20
Ag(001)	GGA	−1.6	0.9	4.23
	LDA	−2.5	−0.03	4.64
	Expt.	0.0 ± 1.5[j]	0.0 ± 1.5[j]	4.22 ± 0.04[c]
				4.42[k]
	LDA[f]	−1.9		4.43
	LDA[l]	−2.2	0.4	4.39
	GGA[g]	−1.9	0.6	4.22
	GGA[m]	−1.6	0.7	4.38
	GGA[n]	−1.8	0.7	

[a]Reference 27.
[b]Reference 28.
[c]Reference 29.
[d]Reference 30.
[e]Reference 31.
[f]Reference 32.
[g]Reference 33.
[h]Reference 34.
[i]Reference 35.
[j]Reference 36.
[k]Reference 37.
[l]Reference 25.
[m]Reference 38.
[n]Reference 39.

good agreement with the experimental data and basically consistent with other *ab initio* calculations.

The optimized geometry for the isolated NH_3 molecule in the GGA (LDA) yields the following results for the molecular structure: $d(\mathrm{NH}) = 1.022$ (1.022) Å and $\beta(\mathrm{HNH}) = 106°$ (107°). These values have to be compared with the experimentally reported values of 1.016 Å and 106.5°, respectively. We also calculated the energy barrier for the inversion of the NH_3 molecule. While the LDA result of 0.197 eV underestimates the experimental barrier (0.250 eV), the GGA value of 0.244 eV is in much better agreement.

B. NH_3 adsorption on Ag surfaces

Structure optimizations were performed for a variety of initial orientations of the NH_3 molecule on each surface. From this extensive set of DFT calculations, NH_3 was found to adsorb with the C_3 axis normal to the surface (with the H atoms pointing away from the surface). This is consistent with the generally accepted idea that the chemical bonding in the NH3-metal system can be related to the occupied nitrogen lone-pair orbital interacting with the metal valence bands.

In order to determine the local adsorption site, the adsorption energy of the NH_3 molecule on the Ag surfaces has been explored by looking for the absolute energy minimum and additional stationary points of the system. To achieve this goal, a set of geometry optimizations have been performed by locating the NH_3 molecule at one of the high-symmetry adsorption sites of each surface, i.e., the *top*, the *bridge*, the *fcc hollow*, and the *hcp hollow* sites for the (111) surface; the *top*, the *short-bridge*, the *long-bridge*, and *hollow* sites for the (110) surface; and the *top*, the *bridge*, and *hollow* sites for the (001) surface. For each site, the NH_3 molecule and the first two substrate layers were allowed to relax to a stationary position. While we find considerable substrate relaxations, if the substrate atoms are kept fixed in their ideal positions we find the same conclusions and the adsorption energy changes only by 3 meV.

The results for the various adsorption sites at the different surfaces are compiled in Table II. The adsorption energy per NH_3 molecule E_{ad} is calculated according to

$$E_{\mathrm{ad}} = E_{\mathrm{Ag}}^{\mathrm{slab}} + E_{\mathrm{NH_3}}^{\mathrm{free}} - E_{\mathrm{NH_3/Ag}}^{\mathrm{slab}}, \tag{1}$$

where the total energies of the adsorbate-substrate system, the clean surface, and the free NH_3 molecule are represented by $E_{\mathrm{NH_3/Ag}}^{\mathrm{slab}}$, $E_{\mathrm{Ag}}^{\mathrm{slab}}$, and $E_{\mathrm{NH_3}}^{\mathrm{free}}$, respectively. According to the definition, E_{ad} can be regarded as the energy required to separate the adsorbed system NH_3/Ag into two noninteracting parts: the Ag surface and NH_3 molecules.

Three main conclusions can be obtained from the presented results: (i) on every surface the favored adsorption site for NH_3 is the top site; (ii) at this site the N-Ag distance of 2.39 Å is practically the same for every surface; and (iii) the adsorption energy for the top site depends on the surface structure: 0.32, 040, and 0.49 eV per molecule for (111), (001), and (110), respectively. We note that the latter value is in very good agreement with experimental data by Thornburg and Madix[40] who showed that ammonia adsorbs without dissociation on clean Ag (110) with a binding energy of 11 Kcal/mol (0.48 eV per molecule). For the (111) surface, two different azimuthal orientations of the NH_3 molecule adsorbed on the top site were tested, corresponding to staggered and eclipsed configurations. Between the limit of our calculations, the adsorption energy remains unchanged when the azimuthal orientation is altered.

There are small structural changes in the adsorbed molecule and substrate. For the (110) surface, for instance, the Ag atom that bonds to the NH_3 molecule moves out of the surface plane by ~0.04 Å, reducing the interlayer relaxation. For the clean (110) surface, within GGA $\Delta d_{12} = -7.7\%$, while it becomes −7.3% when NH_3 is adsorbed on top at a coverage $\Theta = 0.25$. We have simulated also a higher coverage regime using $(\sqrt{3} \times \sqrt{3})R30$ ($\Theta = 0.33$), $p2 \times 1$ ($\Theta = 0.50$), and $(\sqrt{2} \times \sqrt{2})R45$ ($\Theta = 0.50$) periodicities for the

TABLE II. Calculated adsorption energies (E_{ad}) and optimized structural parameters for NH_3 adsorbed on low-index Ag surfaces.

		E_{ad} (eV)	$d_{N\text{-}Ag}$ (Å)	$d_{N\text{-}H}$ (Å)	Δd_{12} (%)
Ag(111)	Top	0.32	2.39	1.021	−0.2
	Bridge	0.16	2.87	1.022	−0.2
	fcc	0.15	2.99	1.023	−0.2
	hcp	0.14	2.98	1.026	−0.2
Ag(110)	Top	0.49	2.39	1.022	−7.3
		0.48[a]			
	Short bridge	0.30	2.92	1.023	−7.4
	Long bridge	0.07	2.91	1.025	−7.8
	Hollow	0.05	3.35	1.025	−7.8
Ag(001)	Top	0.40	2.39	1.021	−1.5
	Bridge	0.22	2.87	1.022	−1.6
	Hollow	0.14	3.10	1.023	−1.6

[a]Experimental result from Ref. 40.

(111), (110), and (001) surfaces, respectively. The adsorption energies and N-Ag distances are shown in Table III. The results for $\Theta=0.25$ are also listed for comparison. The results show that adsorption at top sites is favored also at higher coverage. The adsorption energy decreases significantly, in particular at $\Theta=0.50$, indicating a non-negligible lateral interaction between the NH_3 molecules.

The calculated adsorption energies for the different surfaces are relatively small, indicating at first glance physisorption rather than chemisorption. Even for the top-site adsorp-

TABLE III. Adsorption energy and N-Ag equilibrium distance for NH_3 adsorbed on low-index Ag surfaces at different coverage. The term "endo" means that the adsorption at this site is endothermic.

		$p2\times2$ ($\Theta=0.25$)		$(\sqrt{3}\times\sqrt{3})R30$ ($\Theta=0.33$)	
		E_{ad} (eV)	$d_{N\text{-}Ag}$ (Å)	E_{ad} (eV)	$d_{N\text{-}Ag}$ (Å)
Ag(111)	Top	0.32	2.39	0.27	2.39
	Bridge	0.16	2.87	0.10	2.87
	fcc	0.15	2.99	0.08	2.99
	hcp	0.14	2.98	0.08	2.98
		$p2\times2$ ($\Theta=0.25$)		$p2\times1$ ($\Theta=0.50$)	
		E_{ad} (eV)	$d_{N\text{-}Ag}$ (Å)	E_{ad} (eV)	$d_{N\text{-}Ag}$ (Å)
Ag(110)	Top	0.49	2.39	0.34	2.41
	Short bridge	0.30	2.92	0.18	2.92
	Long bridge	0.07	2.91	Endo	
	Hollow	0.05	3.35	Endo	
		$p2\times2$ ($\Theta=0.25$)		$(\sqrt{2}\times\sqrt{2})R45$ ($\Theta=0.50$)	
		E_{ad} (eV)	$d_{N\text{-}Ag}$ (Å)	E_{ad} (eV)	$d_{N\text{-}Ag}$ (Å)
Ag(001)	Top	0.40	2.39	0.17	2.42
	Bridge	0.22	2.87	0.02	2.85
	Hollow	0.14	3.10	Endo	

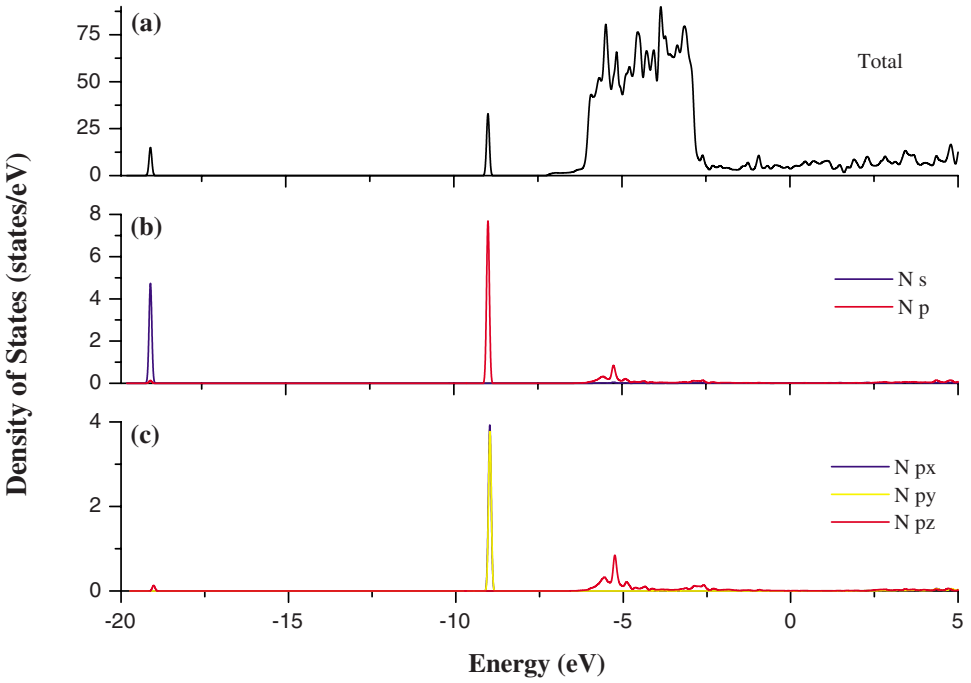

FIG. 1. (Color online) DOS of NH_3 adsorbed on Ag(001). (a) Total. (b) and (c) Projected onto the muffin-tin sphere of nitrogen showing (b) s and p and (c) p_x, p_y, and p_z components.

tion, which is the most stable configuration, the adsorption energies on the different surfaces lie in the range of 0.3–0.5 eV, which is on one hand clearly below the typical values for ionic or covalent bonds, but on the other hand exceeds the known van der Waals interaction energies. The binding mechanism between NH_3 and Ag surfaces is explored by analyzing the electronic properties of the NH_3/Ag slab.

The occupied molecular orbitals (MOs) of free NH_3 are, using Schönflies notation, $(1a_1)(2a_1)(1e)(3a_1)$. Choosing the z axis along the C_3 axis, the N $2p_x$ and $2p_y$ orbitals correspond to the E representation and $2p_z$ to the $A1$ representation. The $3a_1$ orbital has very little hydrogen character and is known as nitrogen $2p_z$ lone-pair orbital of ammonia. The total density of states (DOS) of the NH_3 molecule adsorbed on the Ag(001) surface is shown in Fig. 1(a). The Ag $4d$-band region extends from −6 to −3 eV approximately, while the two sharp peaks centered at −19 and −9 eV correspond to the $2a_1$ and the double degenerate $1e$ orbitals of the NH_3 molecule, respectively. Figures 1(b) and 1(c) display the projection of the density of states on the muffin-tin sphere of nitrogen (s, p, p_x, p_y, and p_z components). These figures reveal that there is a substantial N p_z character in the Ag conduction band, indicating that the orbital of interest is in fact the ammonia $(3a1)$. By examining the components of the Ag d orbitals, it is found that the mixing is mainly with the dz^2. Figure 2 shows the partial density of states for the dz^2 orbital of the Ag atom bonded to the NH_3 molecule, together with the N p_z contribution. This figure reveals a strong hybridization between these two states. As we will see in Sec. III C, the double peak structure of the DOS indicates that the interaction of the ammonia lone-pair orbital with the Ag $4dz^2$ will result in local bonding and antibonding combinations. It is worth pointing out that the energy position of the double peak structure shown in Fig. 2 practically does not depend on the surface structure, indicating that the $4dz^2$ energy level varies very little with facets.

Some insight into the character of the bonding can be gained from the spatial variation of the charge density which can be readily calculated from the DFT wave functions. We calculate the spatially resolved charge-density difference,

$$\Delta\rho(r) = \rho^{NH_3/Ag}(r) - \rho^{Ag}(r) - \rho^{NH_3}(r), \qquad (2)$$

where $\rho^{NH_3/Ag}(r)$, $\rho^{Ag}(r)$, and $\rho^{NH_3}(r)$ are the charge densities of the relaxed adsorbate-substrate system (shown in the left panel of Fig. 3), of the clean surface, and of the adsorbate without substrate, respectively. We note that $\rho^{Ag}(r)$ and $\rho^{NH_3}(r)$ are evaluated using the distorted structure obtained for the NH_3/Ag system. So, there is no charge variation due to displacements of Ag, N, or H atoms. The adsorption-

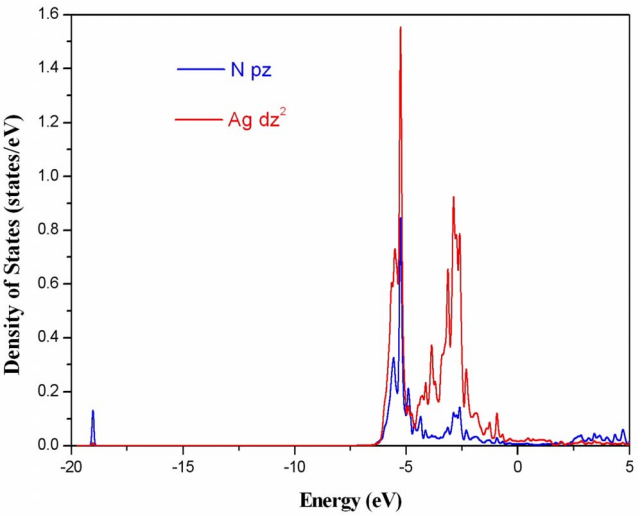

FIG. 2. (Color online) Partial density of states showing the dz^2 contribution of the Ag atom bonded to the NH_3 molecule, together with the N p_z contribution, revealing a strong hybridization between these states.

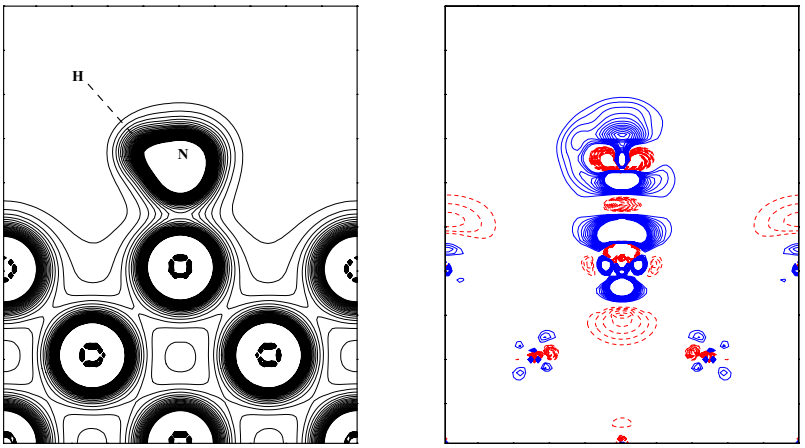

FIG. 3. (Color online) Total electron-density map (left panel) and density difference (right panel) for a cut perpendicular to the Ag(001) surface passing through the N atom of adsorbed NH_3. Regions of electron accumulation (depletion) are displayed in dashed red (solid blue) with isosurface value of $\pm 0.002e/\text{Å}^3$.

induced charge-density difference for the (001) surface is shown in Fig. 3 (right panel). It is clear that the charge-density difference is almost perfectly symmetric about the Ag-N axis, with only a weak modification around the H atom. This picture is very much similar to what one would expect for a local covalent directional bonding of the NH_3 to the single nearest-neighbor Ag atom via the N lone-pair electrons. However, $\Delta\rho(r)$ displays strong sign variations along the N-Ag bond and at the neighbor Ag atoms. A similar picture was obtained for the bond formed between the amino group of adenine and a Cu surface,[15] being an indication that the NH_3 molecule polarizes the Ag substrate.

C. Interactions in $AgNH_3$ and Ag_2NH_3 complexes

It has been shown that the most favorable adsorption site for NH_3 is the top site. This is the most stable configuration for the three examined surfaces and seems to be a general property of the NH_3-Ag interaction. Now we investigate to what extent the formation of this weak chemical bond might be determined by local interactions. To this purpose we studied the simplest model for top bonded ammonia, i.e., NH_3 bonded to a single Ag atom. Then, a second Ag atom is added to incorporate, in a simple manner, the effect of the polarization of the electron density away from the binding site. As pointed out in Sec. II the calculations were carried out also with the WIEN2K package using GGA and spin-polarization corrections.

We summarize first the results of the geometry optimization of the $AgNH_3$ complex, which should be enough to give a qualitative description of the local NH_3-Ag interaction. Varying the N-Ag distance $d_{\text{N-Ag}}$ and the angle between the Ag-N direction and the ammonia C_3 axis we have found that the global potential minimum of the Ag-NH_3 interaction is realized for a C_{3v} symmetric complex where silver faces the nitrogen side. The corresponding equilibrium distance is $d_{\text{N-Ag}}=2.39$ Å, the same value obtained for the three previously investigated surfaces. For the binding energy we obtained $E_b=0.33$ eV, very close to the adsorption energy calculated for the molecule on the (111) surface. The internal structure of NH_3 does not change significantly. A previous quantum-mechanics calculation for the Ag-NH_3 complex reported $E_b=0.26$ eV and $d_{\text{N-Ag}}=2.42$ Å.[17]

The reasonable agreement found between the extended cases and the $AgNH_3$ complex calculation suggests that the interaction between NH_3 and the silver surface is *mainly* of local character. Therefore, the analysis of the bond in this complex should provide additional qualitative insight into the bonding interaction, giving an understanding of the results at a more intuitive level. In Fig. 4, we display the MO diagram corresponding to the NH_3Ag complex for an energy window between 0 and −20 eV. The energy of the HOMO was set to zero. In this energy window there appear four occupied MOs of ammonia: the $2a_1$, the double degenerate $1e$, and the lone-pair $3a_1$ orbitals. The molecular orbitals of the complex have been identified in Fig. 4 as mainly of silver character or of ammonia character through dotted lines, which connect orbitals with similar character. The percentage contribution of these orbitals to the one-electron states has been summarized in Table IV (note that these values depend on the muffin-tin sphere radius, so they must be taken as a

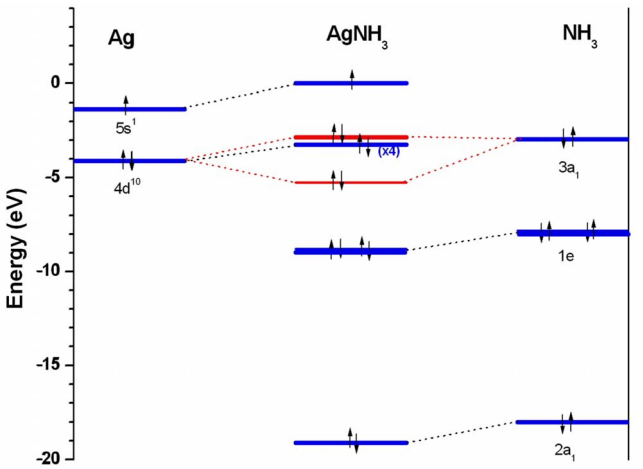

FIG. 4. (Color online) MO-like diagram of the interaction between an isolated Ag atom and a NH_3 molecule. The results correspond to one-electron states associated with the spin up. The energy of the highest occupied molecular orbital (HOMO) of the complex was set to zero. The dotted lines connect orbitals of similar character. The energy levels for bonding and antibonding combinations of N $2p_z$ and Ag $4dz^2$ states (plotted in red) are placed at −5.27 eV and −2.68 eV, respectively.

TABLE IV. Character of the MOs found in the energy window between 0 and −20 eV for the $AgNH_3$ complex. The results correspond to one-electron states associated with the spin up. Note that the values depend on the muffin-tin sphere radius, so the results must be taken as qualitative information.

E (eV)	Ag s (%)	Ag p (%)	Ag d (%)	N s (%)	N p (%)	H s (%)
0	71.5	3.5	9	8	8	0
−2.68	2.3	0.7	90	1	6	0
−3.24 (×4)	0	0	100	0	0	0
−5.27	4	1.4	37.6	4	53	0
−8.80 (×2)	0	0	0.7	0	69.3	30
−19.14	0.1	0.1	0.2	84.6	0	15

qualitative result). We find that there is a considerable overlap between the lone-pair orbital of N and the Ag $4dz^2$ atomic orbital. In fact, the two MOs with energies −5.27 and −2.68 eV are bonding and antibonding combinations of N $2p_z$ and Ag $4dz^2$ states, respectively. These combinations, quantitatively shown as contour plot lines in Fig. 5, manifested as a double peak structure in the DOS plotted in Fig. 2 for the extended surface. We point out that a qualitatively similar MO diagram was obtained for the case of AgH_2O.[41] In that complex, bonding and antibonding combinations of Ag $4dz^2$ and H_2O lone-pair states are formed providing evidence of a covalent contribution to the H_2O-Ag bond. So, the results obtained for the Ag-NH_3 complex provide an additional strong indication that a covalent contribution is important in the characterization of the Ag-N bond. These results, however, cannot explain the different adsorption energies obtained for the three investigated surfaces. The binding energy in the complex is very close to the adsorption energy calculated for the (111) surface, which is the most compact surface of Ag. In contrast, the adsorption energy for the more open (110) surface is ~50% higher. To address this point in a qualitative manner, the effect of the polarization of the electron density away from the binding site is analyzed by the addition of a second Ag atom to the complex.

The ground state of the Ag_2NH_3 complex is found to have the linear end-on C_{3v} structure. The corresponding equilibrium distances are $d_{\text{N-Ag}}$=2.32 Å and $d_{\text{Ag-Ag}}$=2.60 Å. For the binding energy we obtained E_b=0.71 eV, which is in excellent agreement with the experimental value of 0.69 eV reported by Rayner *et al.*[18] The second silver atom in the dimer affords the opportunity to compensate for repulsion in the entrance channel between the N lone pair and the Ag σ electrons by reaccommodation of the electron charge density. We therefore investigated the dependence of the binding energy on the position of the second Ag atom, by changing the Ag-Ag distance ($d_{\text{Ag-Ag}}$) and the angle (θ) between the N-Ag and Ag-Ag bond directions, as illustrated in Fig. 6. This figure shows the binding energy as a function of $d_{\text{Ag-Ag}}$ for different values of θ. The results indicate that E_b depends smoothly on the Ag-Ag distance (for a given value of θ) and strongly varies with the θ angle from ~0.71 eV at θ=0° to ~0.1 eV at θ=90°. This angular dependence is an indication that the atomic position of metal centers around the surface atom bonded to the NH_3 molecule is also important for the characterization of the bond. In the (111) surface, for example, each surface atom has six nearest neighbors in the first layer ($d_{\text{Ag-Ag}}$=2.92 Å, θ=90°) and another three in the layer immediately below ($d_{\text{Ag-Ag}}$=2.91 Å, θ=42°). Although the first layer of the (110) surface is less compact, it has four nearest neighbors in the layer immediately below ($d_{\text{Ag-Ag}}$=2.86 Å, θ=62°) and one directly below it in the third layer ($d_{\text{Ag-Ag}}$=2.84 Å, θ=0°). This, indeed, might explain the different adsorption energies obtained for the three investigated surfaces. While silver atoms belonging to the surface plane (θ=90°) do not provide a strong enough polarization mechanism, the structure of the second and third atomic layers (θ <90°) is indeed relevant to relieve the repulsion between the N lone pair and the Ag electrons by charge reaccommodation.

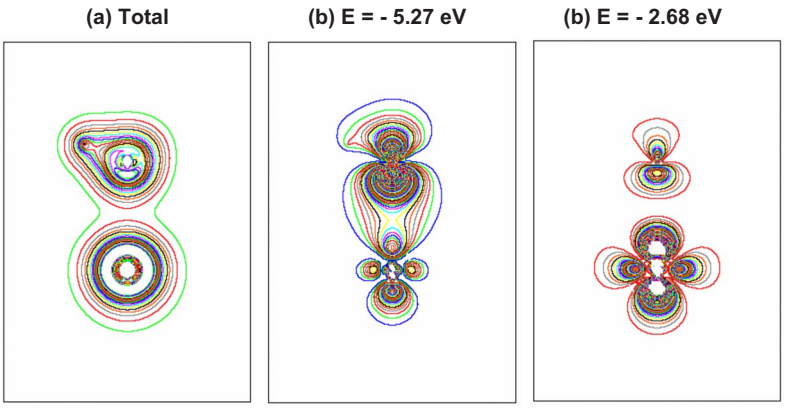

FIG. 5. (Color online) (a) Total charge-density of the NH_3-Ag complex. (b) and (c) Charge-density plots of the MOs with energies −5.27 and −2.68 eV which are bonding and antibonding combinations of N $2p_z$ and Ag $4dz^2$ states, respectively. The spacing between contours is $0.1e/Å^3$ for (a) and $0.02e/Å^3$ for (b) and (c).

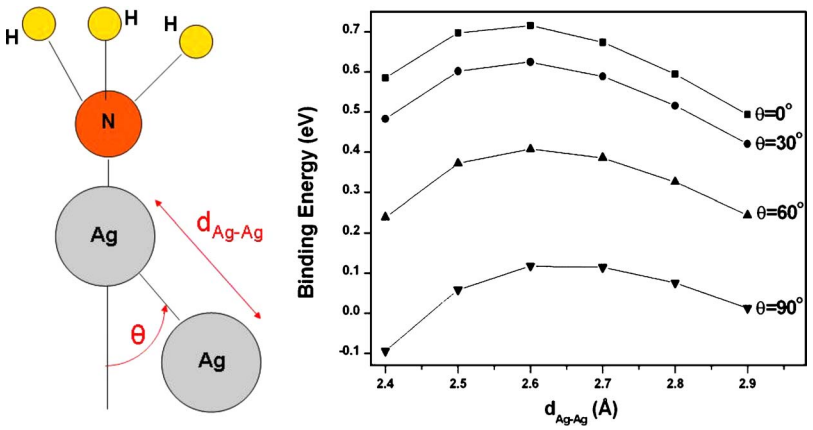

FIG. 6. (Color online) Binding energy for the Ag_2-NH_3 bond as a function of Ag-Ag distance (d_{Ag-Ag}) and angle (θ) between the N-Ag and Ag-Ag bond directions.

IV. CONCLUSIONS

A systematic DFT study has identified a general binding mechanism for NH_3 on Ag surfaces. On all the investigated surfaces, NH_3 adsorbs preferentially at top sites. The N-Ag distance of 2.39 Å is practically the same for all the surfaces. On the other hand, the adsorption energy depends on the surface structure: 0.32, 040, and 0.49 eV per molecule for (111), (001), and (110), respectively.

Our results indicate a significant covalent contribution to the bonding; the adsorption energy cannot be simulated by a simple electrostatic model. The covalent contribution acts via the ammonia lone-pair $3a_1$ orbitals, interacting with the Ag valence $4dz^2$ band. Additionally, the substrate charge density is polarized toward the surrounding metal centers in order to maximize the bonding interaction between the ammonia orbitals and the Ag valence band. So, on the basis of the calculated electronic structure, we explain the bonding as resulting from the combined effects of covalent and polarization contributions. Strain contributions are negligible.

ACKNOWLEDGMENTS

I thank N. Pellegri for suggesting this investigation and R. Migoni for valuable discussions. This research was sponsored by Consejo Nacional de Investigaciones Científicas y Tecnológicas de la Republica Argentina (CONICET) and Consejo de Investigaciones de la Universidad Nacional de Rosario (CIUNR).

[1] A. Nilsson and L. G. M. Pettersson, Surf. Sci. Rep. **55**, 49 (2004).
[2] A. Frattini, N. Pellegri, D. Nicastro, and O. de Sanctis, Mater. Chem. Phys. **94**, 148 (2005).
[3] M. V. Roldán, A. Frattini, O. de Sanctis, H. Troiani, and N. Pellegri, Appl. Surf. Sci. **254**, 281 (2007).
[4] L. Gang, B. G. Anderson, J. van Grondelle, and R. A. van Santen, Appl. Catal., B **40**, 101 (2003).
[5] N. A. Booth, R. Davis, D. P. Woodruff, C. Hirschmugl, K. M. Schindler, O. Schaff, V. Fernandez, A. Theobald, P. Hofmann, A. M. Bradshaw, and V. Fritzsche, Surf. Sci. **387**, 152 (1997).
[6] C. J. Hirschmugl, K.-M. Schindler, O. Schaff, V. Fernandez, A. Theobald, P. Hofmann, A. M. Bradshaw, R. Davis, N. A. Booth, D. P. Woodruff, and V. Fritzsche, Surf. Sci. **352-354**, 232 (1996).
[7] B. Afsin, P. R. Davies, A. Pashusky, M. W. Roberts, and D. Vincent, Surf. Sci. **284**, 109 (1993).
[8] G. J. C. S. van de Kerkhof, W. Biemolt, A. P. J. Jansen, and R. A. van Santen, Surf. Sci. **284**, 361 (1993).
[9] W. Biemolt, G. J. C. S. van de Kerkhof, P. R. Davies, A. P. J. Jansen, and R. A. van Santen, Chem. Phys. Lett. **188**, 477 (1992).
[10] W. Biemolt, A. P. J. Jansen, M. Neurock, G. J. C. S. van de Kerkhof, and R. A. van Santen, Surf. Sci. **287-288**, 183 (1993).
[11] P. S. Bagus and K. Hermann, Phys. Rev. B **33**, 2987 (1986).
[12] P. S. Bagus, K. Herman, and C. W. Bauschlicher, J. Chem. Phys. **81**, 1966 (1984).
[13] J. Hasselström, A. Föhlisch, O. Karis, N. Wassdahl, M. Weinelt, A. Nilsson, M. Nyberg, L. G. M. Pettersson, and J. Stöhr, J. Chem. Phys. **110**, 4880 (1999).
[14] J. Robinson and D. P. Woodruff, Surf. Sci. **498**, 203 (2002).
[15] M. Preuss, W. G. Schmidt, and F. Bechstedt, Phys. Rev. Lett. **94**, 236102 (2005).
[16] H.-H. Ritze and W. Radloff, Chem. Phys. Lett. **250**, 415 (1996).
[17] P. Archirel, V. Dubois, and P. Maıtre, Chem. Phys. Lett. **323**, 7 (2000).
[18] D. M. Rayner, L. Lian, R. Fournier, S. A. Mitchell, and P. A. Hackett, Phys. Rev. Lett. **74**, 2070 (1995).
[19] L. Lian, S. A. Mitchell, P. A. Hackett, and D. M. Rayner, J. Chem. Phys. **104**, 5338 (1996).
[20] J. P. Perdew, K. Burke, and M. Ernzerhof, Phys. Rev. Lett. **77**, 3865 (1996).
[21] D. J. Singh, *Plane Waves, Pseudopotentials and LAPW Method* (Kluwer, Boston/Academic, London, 1994).
[22] P. Blaha, K. Schwarz, G. K. H. Madsen, D. Kvasnicka, and J. Luitz, *WIEN2K: An Augmented Plane Wave + Local Orbitals Program for Calculating Crystal Properties* (Karlheinz Schwarz, Technische Universität Wien, Austria, 2001).
[23] A. Khein, D. J. Singh, and C. J. Umrigar, Phys. Rev. B **51**, 4105 (1995).

[24] K. Doll and N. M. Harrison, Phys. Rev. B **63**, 165410 (2001).
[25] B. D. Yu and M. Scheffler, Phys. Rev. B **55**, 13916 (1997).
[26] B. Medasani, Y. H. Park, and I. Vasiliev, Phys. Rev. B **75**, 235436 (2007).
[27] R. J. Culbertson, L. C. Feldman, P. J. Silverman, and H. Boehm, Phys. Rev. Lett. **47**, 657 (1981).
[28] P. Statiris, H. C. Lu, and T. Gustafsson, Phys. Rev. Lett. **72**, 3574 (1994).
[29] M. Chelvayohan and C. H. B. Mee, J. Phys. C **15**, 2305 (1982).
[30] F. Soria, J. L. Sacedon, P. M. Echenigire, and D. Titherington, Surf. Sci. **68**, 448 (1977).
[31] E. A. Soares, G. S. Leatherman, R. D. Diehl, and M. A. van Hove, Surf. Sci. **468**, 129 (2000).
[32] M. Methfessel, D. Hennig, and M. Scheffler, Phys. Rev. B **46**, 4816 (1992).
[33] H. Fu, L. Jia, W. Wang, and K. Fan, Surf. Sci. **584**, 187 (2005).
[34] Y. Kuk and L. C. Feldman, Phys. Rev. B **30**, 5811 (1984).
[35] H. L. Davis and J. R. Noonan, Surf. Sci. **126**, 245 (1983).
[36] H. Li, J. Quinn, Y. S. Li, D. Tian, F. Jona, and P. M. Marcus, Phys. Rev. B **43**, 7305 (1991).
[37] K. Giesen, F. Hage, F. J. Himpsel, H. J. Riess, W. Steinmann, and N. V. Smith, Phys. Rev. B **35**, 975 (1987).
[38] M. Gajdos, A. Eichler, and J. Hafner, Surf. Sci. **531**, 272 (2003).
[39] S. Clarke, G. Bihlmayer, and S. Blugel, Phys. Rev. B **63**, 085416 (2001).
[40] D. Thornburg and R. Madix, Surf. Sci. **220**, 268 (1989).
[41] V. A. Ranea, A. Michaelides, R. Ramirez, J. A. Verges, P. L. de Andres, and D. A. King, Phys. Rev. B **69**, 205411 (2004).